J|A|C|S
ARTICLES
Published on Web 04/15/2004

Electronic Band Structure of Titania Semiconductor Nanosheets Revealed by Electrochemical and Photoelectrochemical Studies

Nobuyuki Sakai, Yasuo Ebina, Kazunori Takada, and Takayoshi Sasaki*

Contribution from Advanced Materials Laboratory, National Institute for Materials Science, 1-1 Namiki, Tsukuba, Ibaraki 305-0044, Japan

Received November 6, 2003; E-mail: sasaki.takayoshi@nims.go.jp

Abstract: Electrochemical and photoelectrochemical studies were conducted on self-assembled multilayer films of titania nanosheets on a conductive ITO substrate. Cyclic voltammogram (CV) curves indicated that the titania nanosheet electrode underwent insertion/extraction of Li^+ ions into/from the nanosheet galleries, associated with reduction/oxidation of Ti^{4+}/Ti^{3+}. These processes accompanied reversible changes in UV−vis absorption of the titania nanosheet electrodes. Applying a negative bias of −1.3 V (vs Ag/Ag^+) and lower brought about absorption reduction where the wavelength is shorter than 323 nm, and vice versa, indicating a flat-band potential of (approximately) −1.3 V and a band gap energy of 3.84 eV. Photocurrents were generated from the titania nanosheet electrodes under a positive bias. The onset potential for photocurrent generation from the titania nanosheet electrodes was around −1.27 V, and the band gap energy estimated from the photocurrent action spectra was 3.82 eV, in excellent agreement with the values obtained from the spectroelectrochemical data. The lack of difference in the band gap energies for titania nanosheet electrodes with different numbers of layers suggests that a nanosheet is electronically isolated in multilayer assemblies without affecting the electronic state of neighboring nanosheets. Similar measurements on the anatase-type TiO_2 electrode revealed that the lower edge of the conduction band for the titania nanosheet is approximately 0.1 V higher than that for anatase, while the upper edge of the valence band is 0.5 V lower.

Introduction

Photochemistry of semiconductor electrodes is one of the most important topics in fields such as environmental purification and solar energy conversion.[1−4] In these applications, titanium dioxide is strongly favored and has been investigated intensively since Fujishima and Honda discovered water photolysis on TiO_2 semiconductor electrodes.[5] Recently, nanosized TiO_2 materials have attracted growing attention because of their promising potential for a wide range of applications, including photocatalysis[6−12] and dye-sensitized solar cells.[13,14]

We recently synthesized a new modification of nanosized titanium oxide by delaminating precursor crystals of layered titanates into their elementary layers.[15,16] The obtained material has been named titania nanosheets on the basis of its two-dimensional morphology, as depicted in Figure 1. The crystallite has an extremely small thickness of 0.7 nm and a lateral size ranging from submicrometers to several tens of micrometers.[17] The nanosheet may provide new clues in examining various reactions at the surface and interface because nanosheet crystallite is considered to be composed entirely of surface atoms arranged two-dimensionally in a single-crystal-like order. These unusual structural features are expected to evolve novel chemical and physical properties that differ from those for granular titanium oxides. It is of significant interest from a fundamental viewpoint to clarify the electronic band structure for a two-dimensional nanoscopic system of semiconductors, which, to the best of our knowledge, is not yet available. In addition to the titania nanosheets, a variety of semiconducting nanosheet materials, e.g., $Ca_2Nb_3O_{10}$[18,19] and Nb_6O_{17},[20] have recently been synthesized. Such information will provide deep insight in

* To whom correspondence should be addressed. Fax: +81-29-854-9061.

(1) Bard, A. J. *Science* **1980**, *207*, 139−144.
(2) Bard, A. J. *J. Phys. Chem.* **1982**, *86*, 172−177.
(3) Gerischer, H. *Electrochim. Acta* **1990**, *35*, 1677−1699.
(4) Tryk, D. A.; Fujishima, A.; Honda, K. *Electrochim. Acta* **2000**, *45*, 2363−2376.
(5) Fujishima, A.; Honda, K. *Nature* **1972**, *238*, 37−38.
(6) Fox, M. A.; Dulay, M. T. *Chem. Rev.* **1993**, *93*, 341−357.
(7) Heller, A. *Acc. Chem. Res.* **1995**, *28*, 503−508.
(8) Hagfeldt, A.; Grätzel, M. *Chem. Rev.* **1995**, *95*, 49−68.
(9) Hoffmann, M. R.; Martin, S. T.; Choi, W.; Bahnemann, D. W. *Chem. Rev.* **1995**, *95*, 69−96.
(10) Linsebigler, A. L.; Lu, G.; Yates, J. T., Jr. *Chem. Rev.* **1995**, *95*, 735−758.
(11) Mills, A.; Le Hunte, S. *J. Photochem. Photobiol. A* **1997**, *108*, 1−35.
(12) Fujishima, A.; Rao, T. N.; Tryk, D. A. *J. Photochem. Photobiol. C* **2000**, *1*, 1−21.
(13) O'Regan, B.; Grätzel, M. *Nature* **1991**, *353*, 737−740.
(14) Grätzel, M. *Nature* **2001**, *414*, 338−344.
(15) Sasaki, T.; Watanabe, M.; Hashizume, H.; Yamada, H.; Nakazawa, H. *J. Am. Chem. Soc.* **1996**, *118*, 8329−8335.
(16) Sasaki, T.; Watanabe, M. *J. Am. Chem. Soc.* **1998**, *120*, 4682−4689.
(17) Sasaki, T.; Ebina, Y.; Kitami, Y.; Watanabe, M.; Oikawa, T. *J. Phys. Chem. B* **2001**, *105*, 6116−6121.
(18) Xu, F.-F.; Ebina, Y.; Bando, Y.; Sasaki, T. *J. Phys. Chem. B* **2003**, *107*, 9638−9645.
(19) Xu, F.-F.; Ebina, Y.; Bando, Y.; Sasaki, T. *J. Phys. Chem. B* **2003**, *107*, 6698−6703.
(20) Miyamoto, N.; Yamamoto, H.; Kaito, R.; Kuroda, K. *Chem. Commun.* **2002**, 2378−2379.

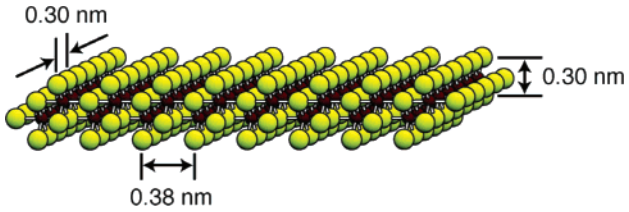

Figure 1. Atomic architecture of the nanosheet crystallites of $Ti_{1-\delta}O_2^{4\delta-}$. Red and yellow circles represent Ti and O atoms, respectively.

physics and chemistry for such an intriguing class of nanoscale two-dimensional semiconductors.

In practice, titania nanosheets exhibit very sharp and intense absorption of ultraviolet (UV) light, which is markedly blue-shifted from that for bulk TiO_2.[21] The nanosheets show photochemical reactivities under UV irradiation, i.e., photocatalytic decomposition of organic substances and photoinduced hydrophilicity.[22] We have demonstrated that a variety of useful materials can be tailored via spontaneous aggregation or self-assembly of the titania nanosheets due to their chemical nature as polyelectrolytes and colloids. For example, ultrathin multilayer films can be fabricated via layer-by-layer assembly of the nanosheets and cationic polymers.[23,24] We expect that some nanostructured systems with sophisticated functions such as efficient photoelectric energy conversion and photocatalytic activities may be designed through synthetic routes. Knowledge on fundamental semiconductor characteristics, e.g., band gap energy and flat-band potential, is essential to achieve this goal.

In the present study, electrochemical and photoelectrochemical properties of the titania nanosheets were explored in order to understand their electronic band structure. Similar measurements were carried out on anatase electrodes prepared by annealing the ultrathin multilayer film of the nanosheets. The electronic band structure for these two very different modifications of titanium oxide, nanosheet and anatase, is compared and discussed below.

Experimental Section

All chemicals were of >99.9% purity or of analytical grade. Polyethylenimine (PEI, $M_w = \sim 7.5 \times 10^5$) and polydiallyldimethylammonium (PDDA, $M_w = \sim 1 \times 10^5$ to 2×10^5) chloride were obtained from Aldrich Co. and used without further purification. Ultrapure water, filtered by a Milli-Q reagent water system at a resistivity of >17 MΩ cm, was used throughout the experiments. Propylene carbonate (Aldrich, H_2O content < 0.002%) containing 0.1 mol dm^{-3} $LiClO_4$ (Wako, anhydrous) was dried for several days using molecular sieves (Wako, 3A).

Titania nanosheets of composition $Ti_{1-\delta}O_2^{4\delta-}$ ($\delta = 0.09$) were synthesized by delaminating a layered protonic titanate with the γ-FeOOH-type structure into colloidal single layers according to previously reported procedures.[15,16] Briefly, a stoichiometric mixture of Cs_2CO_3 and TiO_2 was calcined at 800 °C for 20 h to produce a precursor cesium titanate, $Cs_{0.7}Ti_{1.825}\square_{0.175}O_4$ (□: vacancy), about 70 g of which was treated with 2 dm^3 of a 1 mol dm^{-3} HCl solution at room temperature. This acid leaching was repeated three times by renewing the acid solution every 24 h. The resulting acid-exchanged product was filtered, washed with water, and air-dried.

The obtained protonic titanate, $H_{0.7}Ti_{1.825}\square_{0.175}O_4 \cdot H_2O$, was shaken vigorously with a 0.017 mol dm^{-3} tetrabutylammonium hydroxide solution at ambient temperature for 10 days. The solution-to-solid ratio was adjusted to 250 cm^3 g^{-1}. This procedure yielded a stable colloidal suspension with an opalescent appearance. In our previous study,[17] we demonstrated that this suspension contains unilamellar crystallites of $Ti_{1-\delta}O_2^{4\delta-}$ ($\delta = 0.09$) with a lateral size of 0.1−1 μm.

Indium−tin oxide (ITO)-coated glass plates (sheet resistance = 10 Ω/□) employed as a substrate were cleaned by sonication in acetone, ethanol, and ultrapure water for 30 min each and stored in water until use. The substrate was pretreated with a PEI solution (2.5 g dm^{-3}, pH 9) for 20 min to introduce positive charges onto the surface, immediately prior to film deposition. The titania nanosheets and PDDA were sequentially adsorbed from the colloidal suspension of $Ti_{1-\delta}O_2^{4\delta-}$ (0.08 g dm^{-3}, pH 9) and a PDDA solution (20 g dm^{-3}, pH 9), respectively. The substrate was immersed in each solution for 20 min and then rinsed meticulously with ultrapure water. Deposition of the PDDA/nanosheet bilayer was repeated n times to synthesize a multilayer assembly composed of n layer pairs, ITO/PEI/$Ti_{1-\delta}O_2$/(PDDA/$Ti_{1-\delta}O_2$)$_{n-1}$. The samples were irradiated by UV white light from a Xe lamp (XEF-501S, San-Ei Electric) with its intensity set to 4 mW/cm^2 for 48 h to decompose the polyelectrolytes via photocatalytic action of the titania nanosheets.

Electrochemical and photoelectrochemical measurements were carried out in a conventional three-electrode, single-compartment glass cell, fitted with a synthesized quartz window, using a potentiostat (model SI 1287, Solartron). Titania nanosheet electrodes served as the working electrode. The counter and reference electrodes were platinum black wire and Ag/Ag^+/acetonitrile, respectively. Propylene carbonate containing 0.1 mol dm^{-3} $LiClO_4$ was employed as the supporting electrolyte. A 500 W Xe lamp was used as the excitation light source through a monochromator (H-10UV, Jobin Yvon) to obtain monochromatic light (fwhm = 15 nm). The irradiated light intensity was monitored by a spectroradiometer (USR-30, Ushio) that was calibrated by chemical actinometry.[25] All electrode potential values are given with respect to Ag/Ag^+ (= +0.49 V vs NHE) in the present paper.

X-ray diffraction (XRD) data were collected using a Rigaku RINT-2200 powder diffractometer with graphite monochromatized Cu Kα radiation ($\lambda = 0.154\ 05$ nm). A spectrophotometer (U-4000, Hitachi) equipped with an integrating sphere detection system was employed to record UV−vis absorption spectra for films on ITO/quartz glass substrates. All measurements were conducted under ambient conditions.

Results and Discussion

Film Fabrication. The film assembly on the ITO-coated quartz glass substrate could be followed by UV−vis absorption spectra recorded using blank data of the ITO-coated quartz glass as background. UV−vis absorption spectra obtained were similar to the data for films on a quartz glass substrate,[23,24] except for a small peak at around 400 nm and a shoulder at around 310 nm. The absorption band centered at 262 nm is characteristic of titania nanosheets, and its progressive enhancement as a function of the layer pair number supports the successful multilayer buildup, as shown in Figure 2. The features at 310 and 400 nm could be attributed to interference effects of thin films. The ITO substrate has a thickness of ~200 nm and shows interference fringes in visible light regions, which varies with different numbers of coated layers of titania nanosheets.

A broad XRD peak was observed at $2\theta = 7.0°$ for the as-deposited film, indicating a nanostructure arising from the

(21) Sasaki, T.; Watanabe, M. *J. Phys. Chem. B* **1997**, *101*, 10159−10161.
(22) Sasaki, T.; Ebina, Y.; Fukuda, K.; Tanaka, T.; Harada, M.; Watanabe, M. *Chem. Mater.* **2002**, *14*, 3524−3530.
(23) Sasaki, T.; Ebina, Y.; Watanabe, M.; Decher, G. *Chem. Commun.* **2000**, 2163-2164.
(24) Sasaki, T.; Ebina, Y.; Tanaka, T.; Harada, M.; Watanabe, M.; Decher, G. *Chem. Mater.* **2001**, *13*, 4661−4667.

(25) Number of incident photons was counted by measuring the absorbance of an aqueous solution of Fe^{2+}-1,10-phenanthroline complexes. Upon exposure of the $K_3Fe(C_2O_4)_3$ aqueous solution to monochromatic light, the photoreduction of Fe^{3+} to Fe^{2+} proceeds quantitatively with the number of absorbed photons. The addition of excess 1,10-phenanthroline promotes the complex formation, binding to the photoreduced Fe^{2+} in the solution.

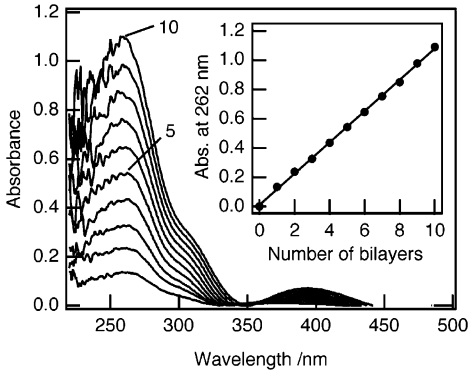

Figure 2. UV−vis absorption spectra for multilayer films of PEI/$Ti_{1-\delta}O_2$/(PDDA/$Ti_{1-\delta}O_2$)$_{n-1}$ prepared on an ITO/quartz glass substrate. Nanosheet concentration = 0.08 g dm^{-3}; pH value of all solutions = 9; deposition time = 20 min each. The observed absorbance at 262 nm is plotted against the number of bilayers in the inset.

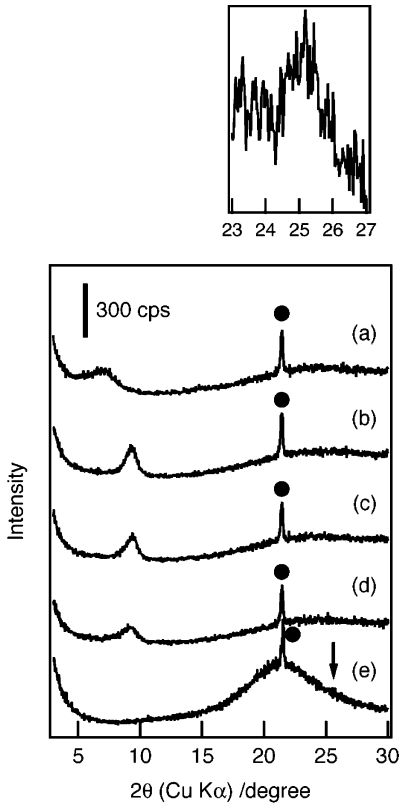

Figure 3. XRD patterns for a 10 layer film of titania nanosheets; (a) as-grown, (b) after UV pretreatment, (c) after photocurrent flow of 5 mC cm^{-2}, (d) after CV measurements for 500 cycles between −1.5 and 1.0 V, and (e) after annealing at 600 °C for 1 h in air. The peak designated by a circle is from ITO. Inset shows a profile in an angular range designated by an arrow in line e.

repeating unit of PDDA/$Ti_{1-\delta}O_2$ (Figure 3a). The multilayer spacing of 1.3 nm agrees with a previously reported value for the same layer-by-layer assembly on a substrate of quartz glass or silicon wafer.[23,24] Exposure of the multilayer film to UV light brought about a shift of the basal peak to a higher 2θ, indicating a periodicity of 0.94 nm (Figure 3b). This intersheet shrinkage has been explained as degradation of the polymer layer via photocatalytic activity of the nanosheets.[22] We have demonstrated that the UV-treated film accommodates charge-balancing cations such as ammonium and/or oxonium ions in the intersheet galleries. We used such polymer-free multilayer films of titania

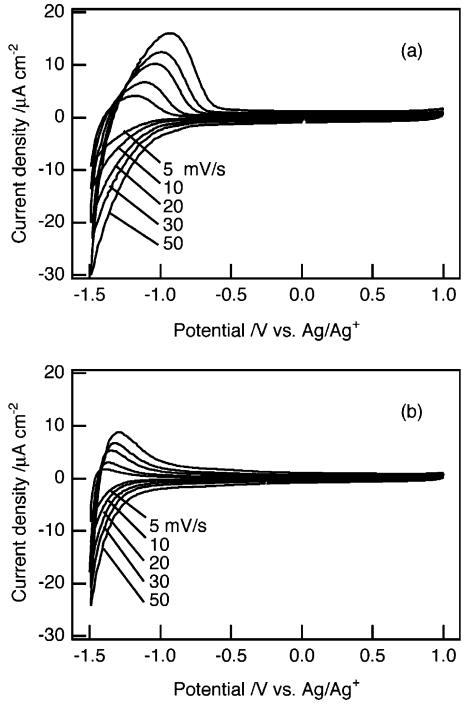

Figure 4. Cyclic voltammograms of a 10 layer film of titania nanosheet electrodes: (a) after UV pretreatment and (b) after annealing at 600 °C for 1 h. CV measurements were conducted in a propylene carbonate solution containing 0.1 mol dm^{-3} $LiClO_4$ at each sweep rate.

nanosheets in the following electrochemical and photoelectrochemical experiments to avoid possible interference with polyelectrolytes. The peak position remained unchanged after photocurrent generation (5 mC cm^{-2} flowed at 0.1 V under monochromatic light irradiation centered at 280 nm) and CV measurements for 500 cycles (between −1.5 and 1.0 V, sweep rate = 50 mV s^{-1}), respectively, except for some line broadening (Figures 3c and 3d). These data confirm the substantial stability of the nanosheet architecture as well as the multilayer structure against electrochemical and photoelectrochemical processes.

Anatase film was prepared for reference use by annealing the 10 layer film of titania nanosheets at 600 °C for 1 h in air. As shown in Figure 3e, the basal peak disappeared, reflecting the collapse of the multilayer structure. Anatase crystallized in its place,[26] as revealed by the 101 peak that appeared around $2\theta = 25.2°$ shown in the inset at an expanded scale. The sharp peak observed at a 2θ of 21.4° and the halo pattern observed at 15−30° can be assigned to the ITO and the quartz glass of its substrate,[27] respectively.

Electrochemistry. Electrochemical studies of the titania nanosheet electrodes and anatase electrodes were carried out in nonaqueous electrolyte. As depicted in Figure 4a, the cyclic voltammogram of the 10 layer film of titania nanosheet electrode showed a poorly resolved cathodic peak and a well-defined anodic peak, which is centered at around −1.2 to −0.9 V. These peaks can be accounted for by the reduction/oxidation of the

(26) To detect diffraction peaks from a very thin film of anatase, we conducted glancing incidence XRD at a constant incident angle of 0.8° using Cu Kα radiation operated at 40 kV and 400 mA. The obtained profile is shown in the inset of Figure 3.

(27) ITO films coated on quartz glass were employed as substrates in preparation of the anatase electrodes because ITO substrate for normal glass may not be stable upon annealing at 600 °C. XRD data suggested that ITO films themselves remained unchanged, although the sheet resistance increased from 10 to 30 Ω/□.

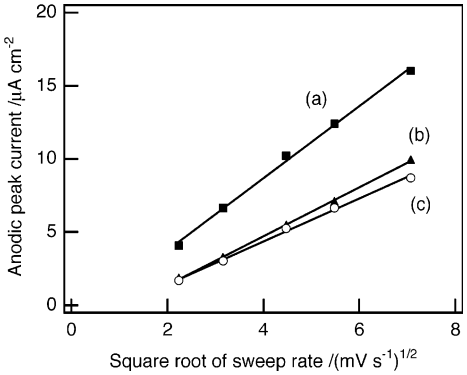

Figure 5. Dependence of the anodic peak current on the square root of the sweep rate: (a) 10 and (b) 5 layer films of titania nanosheet electrodes and (c) anatase electrode.

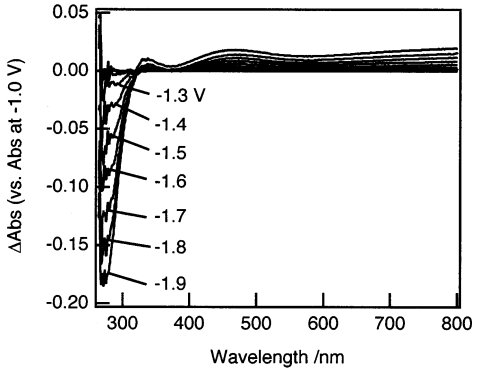

Figure 6. UV−vis absorption spectra for a 10 layer film of titania nanosheet electrodes under various bias. The baseline is the absorbance of the titania nanosheet electrode at −1.0 V.

titania nanosheet, accompanying insertion/extraction of Li^+ ions into/from the titania nanosheet galleries.

$$(NH_4, H)_{4\delta}Ti^{IV}{}_{1-\delta}O_2 + x(Li^+ + e^-) \rightleftarrows Li_x(NH_4, H)_{4\delta}Ti^{III}{}_xTi^{IV}{}_{1-\delta-x}O_2 \quad (1)$$

This process can be understood as the intercalation/deintercalation of Li^+ ions into/from the interlayer space where charge-compensating cations (NH_4^+, H_3O^+) are present. The oxidation peak current for the 10 layer film electrode was almost twice that of the 5 layer sample, reflecting equivalent and electroactive intersheet environments in the multilayer film. The linear relationship between the oxidation peak current and the square root of the potential sweep rate (Figure 5) suggests that the diffusion of Li^+ ions is a rate-determining step in oxidation of Ti^{3+} in the titania nanosheet. Reduction of a trace amount of water dissolved in the electrolyte and persisting in the nanosheet galleries may be responsible for nonzero intercepts of the straight lines and a negative baseline for the oxidation peak. The integration of the oxidation peak observed at a sweep rate of 5 mV/s gave the amount of Ti^{3+} of 123 μC cm^{-2} at −1.5 V. Because the two-dimensional unit cell of the nanosheet crystallite (0.38 × 0.30 nm^2) contains two formula weights of $Ti_{1-\delta}O_2$, the 10 layer film has 1.60 × 10^{15} Ti atom cm^{-2} if we assume a perfect film without gap or overlap of the nanosheets. Accordingly, the electrochemical process described above involves reduction/oxidation of 4.8% of Ti atom. Sweeping the potential to −2.0 V induced a deeper reduction/oxidation degree of ∼50%, i.e., 0.5 for x in eq 1. This corresponds to the accommodation of one Li ion per unit cell of the nanosheet.

The anatase electrode showed a similar CV profile, but redox peaks were smaller than those of the titania nanosheet electrode, as shown in Figures 4b and 5c. The oxidation peaks obtained at 5 mV s^{-1} had a peak area of 45.5 μC cm^{-2}. The smaller redox peak area may be attributable to a structural difference. Li^+ ions are inserted into interstitial voids in the three-dimensional framework of the anatase structure. This feature hinders insertion into the deep inner portion of the crystallite; Li^+ ions likely exist only near the surface.[28,29] In contrast, the nanosheet electrode accommodates Li^+ ions in the intersheet space, which has a larger number of available sites with more facile accessibility.

The redox processes in eq 1 induced a change in the UV−vis absorption of the titania nanosheet electrodes associated with the redox Ti^{4+}/Ti^{3+} couple. Similar electrochromic behavior has been reported for polycrystalline anatase.[30−36] Optical absorption spectra of the titania nanosheet electrode were recorded following polarization for 60 s at various applied potentials. The electrode potential was changed from the rest potential in the negative direction at a step of 0.1 V. Absorption enhancement and reduction where the wavelength is longer and shorter than 323 nm, respectively, were observed under a negative bias at −1.3 V and lower, as shown in Figure 6. The absorption enhancement at λ > 323 nm can be ascribed to intraband transitions by electrons occupying the conduction band states of the titania nanosheet,[37] whereas the absorption reduction at λ < 323 nm can be accounted for by the apparent increase in the band gap energy due to electron accumulation in the conduction band states (Burstein shift).[37,38] Therefore, the onset potential for the change in optical absorption corresponds to the flat-band potential and the border wavelength between the absorption enhancement and reduction corresponds to the band gap energy. The absorbance change at 800 and 275 nm measured for each potential vs −1.0 V as a reference was plotted against the applied potential (Figure 7). The decrease of the absorbance at 275 nm for both 5 and 10 layer films was observed at −1.3 V and lower. The plots between −1.3 and −2.0 V could be fitted with a straight line for each layer number of films.[39] From the intersecting point of these two straight lines, a threshold potential of −1.27 V (Δabs = −0.003) was obtained. The absorbance change at 800 nm, which is proportional to the density of electrons in the conduction band,[30] also gives the

(28) Kavan, L.; Grätzel, M.; Gilbert, S. E.; Klemenz, C.; Scheel, H. J. *J. Am. Chem. Soc.* **1996**, *118*, 6716−6723.
(29) van de Krol, R.; Goossens, A.; Schoonman, J. *J. Phys. Chem. B* **1999**, *103*, 7151−7159.
(30) Rothenberger, G.; Fitzmaurice, D.; Grätzel, M. *J. Phys. Chem.* **1992**, *96*, 5983−5986.
(31) Redmond, G.; Fitzmaurice, D. *J. Phys. Chem.* **1993**, *97*, 1426−1430.
(32) Kavan, L.; Stoto, T.; Grätzel, M.; Fitzmaurice, D.; Shklover, V. *J. Phys. Chem.* **1993**, *97*, 9493−9498.
(33) Enright, B.; Redmond, G.; Fitzmaurice, D. *J. Phys. Chem.* **1994**, *98*, 6195−6200.
(34) Boschloo, G.; Fitzmaurice, D. *J. Phys. Chem. B* **1999**, *103*, 7860−7868.
(35) Lyon, L. A.; Hupp, J. T. *J. Phys. Chem. B* **1999**, *103*, 4623−4628.
(36) Sakai, N.; Fujishima, A.; Watanabe, T.; Hashimoto, K. *J. Phys. Chem. B* **2001**, *105*, 3023−3026.
(37) Pankove, J. I. *Optical Processes in Semiconductors*; Prentice-Hall: New Jersey, 1971.
(38) Burstein, E. *Phys. Rev.* **1952**, *93*, 632−633.
(39) The reason for the linear relationships between the absorbance change at 275 nm and the applied potential is not still clear, but it may be related with the density of states of electrons in the titania nanosheets.

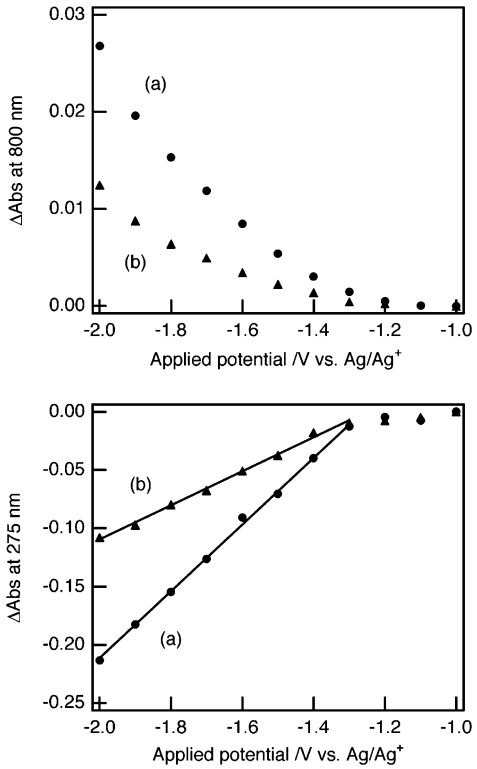

Figure 7. Changes in absorbance at 800 (top) and 275 nm (bottom) for (a) 10 and (b) 5 layer films of titania nanosheet electrodes as a function of the applied potential.

threshold potential by fitting the plots with the distribution function of density of states in the conduction band. However, without data such as the density of states in the conduction band and the donor density of the titania nanosheets, we cannot carry out such a fitting procedure at the moment. The border wavelength of 323 nm corresponds to a photon energy of 3.84 eV. These results lead to the conclusion that the flat-band potential and the band gap of the titania nanosheet electrodes are around −1.27 V and 3.84 eV, respectively. It should be noted that the absorbance changes were linearly dependent on the number of titania nanosheet layers for each applied potential. This result suggests that intercalated Li^+ ions were homogeneously distributed throughout the nanosheet galleries without segregation in the vicinity of the interface with the electrolyte.

Spectroelectrochemical measurements for the anatase electrode were conducted in a similar manner to compare the electronic band structure of titania nanosheets with that for the famous polymorph of TiO_2. In Figure 8, the absorbance differences at 800 and 325 nm measured for each potential vs −0.5 V as a reference are plotted against the applied potential. The absorbance change for anatase was small compared to that for titania nanosheets in accordance with the small redox peaks of CV shown above. Because of this, the precise onset potential for the absorption changes at 800 and 325 nm was difficult to determine. But it is clear that the flat-band potential of the anatase is slightly more positive than that of the titania nanosheets.

Photoelectrochemical Properties. Photoelectrochemical experiments were also conducted in a propylene carbonate solution containing 0.1 mol dm^{-3} $LiClO_4$, which is the same as that in the electrochemical experiments. An anodic photocurrent of significant magnitude (sub-μA cm^{-2}) was observed when the

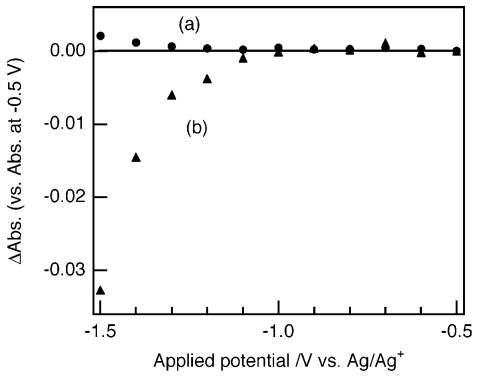

Figure 8. Changes in absorbance at (a) 800 and (b) 325 nm for an anatase electrode as a function of the applied potential.

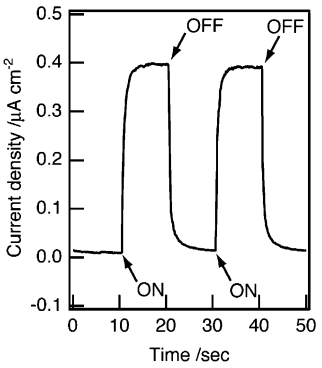

Figure 9. Photocurrent generation from the 10 layer films of titania nanosheet/ITO electrode at 0.1 V under monochromatic light centered at 280 nm.

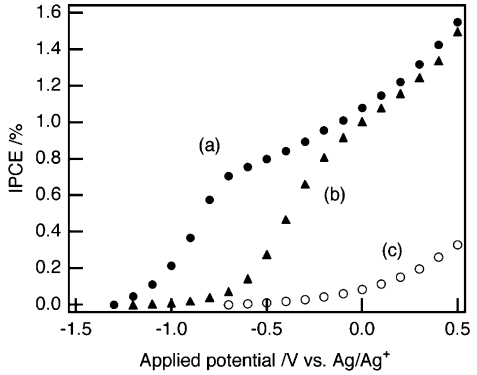

Figure 10. Dependence of the IPCE values on the applied potential: (a) 10 layer film of titania nanosheet electrode, (b) anatase electrode, and (c) bare ITO electrode. The incident light source was monochromatic light centered at 280 nm for a and c, and at 365 nm for b.

titania nanosheet electrode was irradiated with a monochromatic UV light ($\lambda = 280$ nm) at 0.1 V (Figure 9). The onset potential of the anodic photocurrent generation was between −1.3 and −1.2 V, which was determined to be -1.27 ± 0.05 V by more detailed measurements (Figure S1a, Supporting Information). This value agrees well with the flat-band potential obtained by the spectroelectrochemical measurements described above (Figure 10a). Generally, a flat plateau is observed in a potential region away from the photocurrent onset,[40] which was not the case in the present system. The slow increase of the photocurrent under potentials more positive than −0.7 V may be ascribed to the photocurrent generation from the ITO substrate and/or the

(40) Nozik, A. J.; Memming, R. *J. Phys. Chem.* **1996**, *100*, 13061−13078.

small dielectric constant.[41] In contrast, no cathodic photocurrents were observed under potentials more negative than the flat-band potential. These characteristics are typical for n-type semiconductors. A full understanding of the redox reactions of excited electrons and holes associated with photocurrent generation is not available at the present stage. We speculate that the electrons may reduce water and/or molecular oxygen dissolved in the electrolyte, while the holes may oxidize water and/or propylene carbonate used as electrolyte.

Note that the onset potentials of photocurrent generation were the same for the titania nanosheet electrodes with various numbers of layers. This agrees well with the identical onset potential of Li^+ ion intercalation between 5 and 10 layer films of titania nanosheet electrodes, which was observed in the spectroelectrochemical experiments. The reason for these results can be elucidated as follows. The topmost surface structure generally dominates the flat-band potential of the semiconductor electrodes.[40] In the present system, the topmost surface should be identical to the two-dimensional architecture of a titania nanosheet despite differences in the number of layers, so that identical flat-band potentials were observed for various numbers of layers.

Photocurrent generation from the anatase electrodes was also examined under a monochromatic light with a wavelength centered at 365 nm. As shown in Figure 10b and S1b (Supporting Information), the anodic photocurrent was observed at around −1.15 V and more positive potentials. This value is consistent with the flat-band potential obtained in aprotic nonaqueous solvents.[31] These results confirm the shift of the flat-band potential via transformation of the titania nanosheet into anatase.

Figure 11I displays photocurrent action spectra in which the incident photon-to-electron conversion efficiency (IPCE) is plotted as a function of the excitation wavelength. The onset wavelength for photocurrent generation from the titania nanosheet electrode was around 320 nm, which is independent of the number of layers of titania nanosheets, while the IPCE value increased with increasing number of layers, probably due to larger light absorption. The light irradiation ($\lambda < 340$ nm) also allows the bare ITO electrode to generate photocurrent. However, the much higher efficiency for the samples with the nanosheet, as well as the different onset wavelengths, strongly suggests that the photocurrent observed on these films originates from the titania nanosheets.

To estimate the band gap energy for each electrode, the square root of the IPCE times the photon energy, $(\eta h\nu)^{0.5}$, is plotted against photon energy $h\nu$ (Figure 11II).[28] A straight line appears for each multilayer of titania nanosheet electrode in a photon energy range close to the absorption threshold, indicating that the electronic transition near the band gap is indirect. The band gap energies for the 2, 5, and 10 layer films of titania nanosheets are all derived as 3.82 eV from the intercepts of the linear portion of the curves with the abscissa. This value is consistent with that obtained in the spectroelectrochemical experiments. Furthermore, similar analysis on the optical data for the titania nanosheet films, i.e., a plot of $(\alpha h\nu)^{0.5}$ against $h\nu$ (α: absorption coefficient), provided a band gap energy of 3.85 eV. The lack of difference in the band gap energies for titania nanosheet

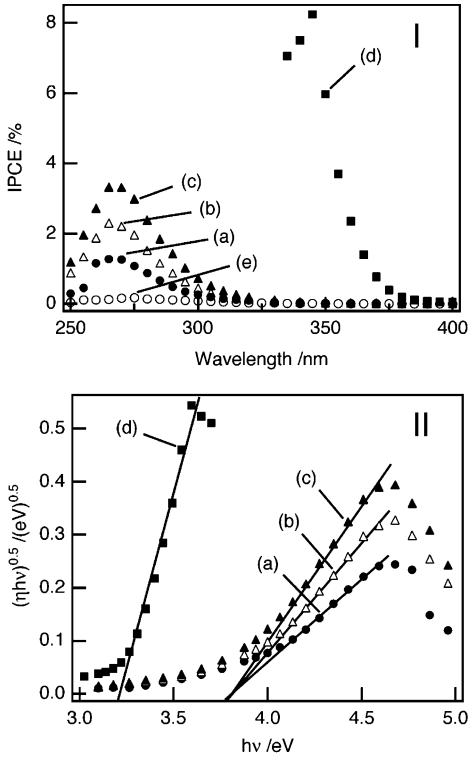

Figure 11. (I) Photocurrent action spectra for (a) 2, (b) 5, and (c) 10 layer films of titania nanosheet electrodes, (d) anatase electrode, and (e) bare ITO electrode. (II) Data replotted for estimation of band gap. The symbols used are the same as for I.

electrodes with different numbers of layers indicates that the nanosheet is electronically isolated in the multilayer assemblies without affecting the electronic state of neighboring nanosheets.

The maximum IPCE for the 10-layer titania nanosheet electrode was calculated to be approximately 3.3% under a monochromatic light ($\lambda = 265$ nm) at 0.1 V. One of the reasons for the relatively low IPCE value lies in the two-dimensional structure, which leads to a higher probability for the excited electron−hole recombination. The excited carriers migrate primarily in two-dimensional directions, unlike other materials such as anatase and rutile where three-dimensional diffusion is allowed. Furthermore, the migration of charge carriers to the ITO substrate inevitably requires hopping from one semiconductor nanosheet to another. A high barrier in the charge transfer between the nanosheets is anticipated, which may also be responsible for attenuation of the IPCE value as discussed below. From the absorption spectra for multilayer films of titania nanosheets, with the assumption that the amount of adsorbed nanosheets is equal in both ITO and quartz sides, the ratio of the absorbed photon number at $\lambda = 262$ nm was obtained as 1:1.95:3.01 for 2, 5, and 10 layer films. In contrast, the ratio of photocurrent magnitude at $\lambda = 265$ nm was 1:1.80:2.60. If the photocurrent is assumed to be proportional only to the number of absorbed photons, the loss of the photocurrent is calculated to be 7.7 and 13.6% for 5 and 10 layer films compared to the case of 2 layer films.

The onset wavelength for photocurrent generation from the anatase electrode was around 385 nm (Figure 11I), being close to values reported for bulk anatase.[28] The average size of anatase crystallite was determined from the full width at half-maximum (fwhm) of the strongest X-ray diffraction peak (101) in the inset

(41) Sato, H.; Ono, K.; Sasaki, T.; Yamagishi, A. *J. Phys. Chem. B* **2003**, *107*, 9824−9828.

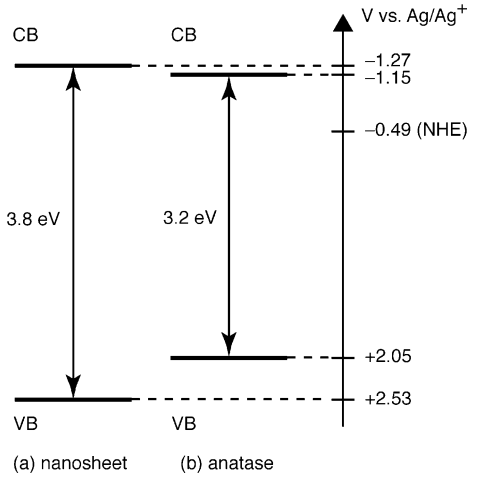

Figure 12. Schematic illustration of electronic band structure: (a) titania nanosheets and (b) anatase.

of Figure 3 using the Scherrer equation, which assumes the small crystallite size to be the only case of line broadening:[42]

$$D = \frac{K\lambda}{\beta\cos\theta} \tag{2}$$

where D is the mean crystallite dimension, K the crystallite shape constant (0.9), θ the Bragg angle, λ the X-ray wavelength, and β the fwhm of the peak in the unit of radians. The calculated size of anatase crystallite was 8.1 nm. It has been established that anatase crystallites of this size exhibit bulk physical properties when the particle diameters are larger than 5 nm.[43,44] In fact, the optical absorption properties of anatase films converted from 10 layer films of titania nanosheets were of bulk nature.[22] The band gap energy of the anatase electrode was also estimated to be 3.2 eV (Figure 11II), which is consistent with that reported for bulk anatase in previous studies.[28,45] The band gap energy of titania nanosheets larger than that of anatase is compatible with the estimation based on the first-principles calculations within density functional theory.[41]

Electronic Structure. On the basis of the results obtained above, the electronic band structure of the titania nanosheet and the anatase can be described as in Figure 12. The band gap energy of the titania nanosheet and the anatase is 3.8 and 3.2 eV, respectively, and the flat-band potential is positioned at −1.27 and −1.15 V.[46] Therefore, the lower edge of the conduction band for the titania nanosheet is 0.1 V higher than that for anatase and the upper edge of the valence band is 0.5 V lower, suggesting that photogenerated electron−hole pairs in the titania nanosheets have stronger reduction and oxidation power than in anatase.

It is of significant interest to discuss the origins of the difference in electronic structure. It is reasonable to presume that a drastic structural variation contributes to the difference, but its value of 0.6 eV may be so large as to be solely ascribed to the structural aspects. In fact, the layered titanate, a precursor material for the titania nanosheets, was reported to have a band gap energy of 3.24 eV based on the estimation by the diffuse reflectance absorption spectrum.[21] This value is smaller by 0.6 eV than that of nanosheets and comparable to that of anatase.

Another plausible explanation for the larger band gap energy of titania nanosheets is quantum size effects[40,47] in a two-dimensional structure with a thickness less than 1 nm. For a two-dimensional crystallites, the band gap shift, ΔE_g, is described by the equation[32,48−50]

$$\Delta E_g = \frac{h^2}{4\mu_{xy}L_{xy}^2} + \frac{h^2}{8\mu_z L_z^2} \tag{3}$$

where μ_{xy} and μ_z are the reduced effective masses of electron−hole pairs in parallel (xy) and perpendicular (z) directions with respect to the anisotropic crystallites ($\mu^{-1} = m^*_e{}^{-1} + m^*_h{}^{-1}$ where m^*_e and m^*_h are the effective mass of the electron and the hole, respectively) and L_{xy} and L_z are the corresponding dimensions of the crystallite. For the nanosheets, L_{xy} (0.1−1 μm) is much larger than L_z ~0.7 nm, so that the first term in eq 3 can be neglected. Taking $\Delta E_g = 0.6$ eV and $L_z = 0.7$ nm, the μ_z value is calculated to be $1.28m_e$, which is smaller than that for anatase ($1.63m_e$[43]). The Bohr radius R of an exciton can be calculated in terms of[51−53]

$$R = \frac{\epsilon h^2}{\mu\pi e^2} \tag{4}$$

where ϵ is the dielectric constant at optical frequencies. The dielectric constant for the titania nanosheet can be estimated to be 9 using the square of the refractive index ($n = 3$ at 300 nm),[24] which is consistent with that obtained by the first-principles calculations.[41] With the values for μ ($1.28m_e$) and ϵ (9), we obtain a value for R of about 0.37 nm from eq 4. The exciton radius for titania nanosheet larger than that for anatase (0.3 nm)[52] indicates that the quantum size effect appears in the titania nanosheet with the larger size compared to the case of anatase. In fact, $2R = 0.74$ nm, larger than the thickness of titania nanosheets (0.7 nm), suggests that photogenerated electron−hole pairs can be physically confined in the titania nanosheets.

The quantum size effects may also explain the negative shift of the flat-band potential of titania nanosheets. The band gap increase is accompanied by a shift of the lower edge of the conduction band to higher energy, while the higher edge of the valence band is displaced to lower energy. Consequently, the flat-band potential moves toward values that are more negative. The magnitude of the edge shift may depend on the values of effective mass of electrons and holes. The smaller the effective mass is, the larger the shift of the band edge is.[52] Since TiO_2 has been reported to have $9m_e$ for m_e* and less than $1m_e$ for

(42) Stokes, A. R. In *X-ray Diffraction by Polycrystalline Materials*; Peiser, H. S., Rooksby, H. P., Wilson, A. J. C., Eds.; The Institute of Physics: London, 1960.
(43) Kormann, C.; Bahnemann, D. W.; Hoffmann, M. R. *J. Phys. Chem.* **1988**, *92*, 5196−5201.
(44) Monticone, S.; Tufeu, R.; Kanaev, A. V.; Scolan, E.; Sanchez, C. *Appl. Surf. Sci.* **2000**, *162*−*163*, 565−570.
(45) Tang, H.; Prasad, K.; Sanjinés, P. E.; Schmid, P. E.; Lévy, F. *J. Appl. Phys.* **1994**, *75*, 2042−2047.
(46) Due to experimental limitations, these values have an ambiguity of ±0.05 V at largest.
(47) Henglein, A. *Chem. Rev.* **1989**, *89*, 1861−1873.
(48) Sandroff, C. J.; Hwang, D. M.; Chung, W. M. *Phys. Rev. B* **1986**, *33*, 5953−5955.
(49) Sandroff, C. J.; Kelty, S. P.; Hwang, D. M. *J. Chem. Phys.* **1986**, *85*, 5337−5340.
(50) Smotkin, E. S.; Lee, C.; Bard, A. J.; Campion, A.; Fox, M. A.; Mallouk, T. E.; Webber, S. E.; White, J. M. *Chem. Phys. Lett.* **1988**, *152*, 265−268.
(51) Elliott, R. J. *Phys. Rev.* **1957**, *108*, 1384−1389.
(52) Enright, B.; Fitzmaurice, D. *J. Phys. Chem.* **1996**, *100*, 1027−1035.
(53) Memming, R. *Semiconductor Electrochemistry*; Wiley−VCH: Weinheim, 2001.

m_h*,[43] the shift of the valence band edge is larger than that of conduction band edge. This seems to be consistent with the results described in the present paper. However, further investigation on effective masses of electrons and holes for titania nanosheets is still required.

Conclusion

This study revealed the electronic band structure of titania nanosheets by electrochemical and photoelectrochemical measurements. Electrochromism was observed under a negative bias at −1.3 V and lower. Photocurrent was generated from the titania nanosheets under the positive potential at around −1.27 V and above upon irradiation with UV light (λ < 320 nm). On the basis of these results, the flat-band potential and the band gap energy were estimated to be −1.27 ± 0.05 V and 3.84 eV, respectively, which are approximately 0.1 V more negative and 0.6 eV larger than the values of anatase-type TiO_2. This information may be useful in applications of titania nanosheets such as photoelectric conversion devices and photocatalysts. Furthermore, the obtained electronic band structure will shed light on the chemistry and physics of molecular semiconductors with two-dimensional nanoscopic architecture.

Acknowledgment. This work has been partly supported by CREST of JST (Japan Science and Technology Agency).

Supporting Information Available: Photocurrent−voltage curve of (a) titania nanosheet and (b) anatase electrodes (PDF). This material is available free of charge via the Internet at http://pubs.acs.org.

JA0394582